Radiation Physics and Chemistry 96 (2014) 92–96

Contents lists available at ScienceDirect

Radiation Physics and Chemistry

journal homepage: www.elsevier.com/locate/radphyschem

A diffusion-free and linear-energy-transfer-independent nanocomposite Fricke gel dosimeter

T. Maeyama [a,*], N. Fukunishi [a], K.L. Ishikawa [b,c,d], T. Furuta [b,1], K. Fukasaku [b,e], S. Takagi [b,f], S. Noda [b], R. Himeno [b], S. Fukuda [g]

[a] Nishina Center for Accelerator-Based Science, RIKEN, 2-1 Hirosawa, Wako, Saitama 351-0198, Japan
[b] Advanced Center for Computing and Communication, RIKEN, 2-1 Hirosawa, Wako, Saitama 351-0198, Japan
[c] Department of Nuclear Engineering and Management, Graduate School of Engineering, The University of Tokyo, 7-3-1 Hongo, Bunkyo-ku, Tokyo 113-8656, Japan
[d] Photon Science Center, Graduate School of Engineering, The University of Tokyo, 7-3-1 Hongo, Bunkyo-ku, Tokyo 113-8656, Japan
[e] Department of Neurosurgery, Himon'ya Hospital, 2-9-5 Minami, Meguro-ku, Tokyo 152-0013, Japan
[f] Department of Mechanical Engineering, Graduate School of Engineering, The University of Tokyo, 7-3-1 Hongo, Bunkyo-ku, Tokyo 113-8656, Japan
[g] Research Center for Charged Particle Therapy, National Institute of Radiological Sciences, 4-9-1 Anagawa, Inage-ku, Chiba 263-8555, Japan

HIGHLIGHTS

- We report a new magnetic-resonance-imaging based nanocomposite Fricke gel dosimeter.
- No diffusion of the radiation products was observed during nine days after the irradiation.
- Gel response faithfully reproduced the carbon beam depth-dose distribution.
- The NC-FG dosimeter exhibited a good linearity up to 800 Gy and suppression of LET effects.

ARTICLE INFO

Article history:
Received 8 July 2013
Accepted 12 September 2013
Available online 20 September 2013

Keywords:
Gel dosimeter
Fricke
LET effects
Nanocomposite
Three dimensional dose distribution
Ion-beam cancer therapy

ABSTRACT

We report a new magnetic-resonance-imaging (MRI) based nanocomposite Fricke gel (NC-FG) dosimeter system, which is free from two main drawbacks of conventional Fricke gel dosimeters, namely, the diffusion of the radiation products and the linear-energy-transfer (LET) dependence of the radiation sensitivity when used for ion beams. The NC-FG dosimeter was prepared by incorporating 1% (w/w) clay nanoparticles into deaerated Fricke gel. We have dosimetrically characterized the NC-FG by using MRI measurements after irradiation with a monoenergetic 290 MeV/nucleon carbon beam. No diffusion of the radiation products was observed during nine days after the irradiation. Moreover, its response faithfully reproduced the depth-dose distribution measured by an ionization chamber, which indicates the absence of the LET dependence. Also, the NC-FG dosimeter exhibited a good linearity up to 800 Gy.

1. Introduction

The ferrous sulfate (Fricke) solution has been used as a reliable chemical radiation dosimeter for more than eighty years (Fricke and Hart, 1966; Fricke and Morse, 1927). Gore et al. (1984) proposed the addition of a gel matrix to the aqueous Fricke dosimeter in order to stabilize the spatial information of radiation-induced oxidation, which can be probed with magnetic resonance imaging (MRI). This has pioneered modern gel dosimetry (Baldock et al., 2010; Schreiner, 2004), a technique that records three dimensional (3D) dose distribution in tissue-equivalent gels.

One of the main drawbacks of Fricke gels, with respect to polymer gel dosimeters, is the diffusion of the ferrous and ferric ions despite the presence of the gel matrix, which eventually destroys the information on dose distribution (Penev and Mequanint, 2013). Another drawback is the decrease in radiation detection sensitivity with the increase in linear energy transfer (LET), which hinders absolute dose determination when used for ion beams. The LET dependence is not unique to Fricke gels but common for virtually all types of 3D dosimeters, as well as for film, scintillation, and semiconductor dosimeters (Karger et al., 2010).

In this paper, we report the successful removal of both of these limitations. We have recently shown that nanoclay addition can suppress radiation product diffusion in dichromate gel dosimeters

* Corresponding author. Tel.: +81 48 467 9463; fax: +81 48 461 5301.
E-mail addresses: maeyama@riken.jp, takuya.maeyama@gmail.com (T. Maeyama).
[1] Present address: Nuclear Science and Engineering Directorate, Japan Atomic Energy Agency, 2-4 Shirakata-Shirane, Tokai-mura, Ibaraki 319-1195, Japan.

0969-806X/$ - see front matter © 2013 Elsevier Ltd. All rights reserved.
http://dx.doi.org/10.1016/j.radphyschem.2013.09.004

(Maeyama et al., 2012; Maeyama et al., 2013; Taylor et al., 2013). Inspired by this, in the present study, we incorporated clay nanoparticles called Laponite XLG (Rockwood, 2013) into Fricke gel dosimeters. This nanocomposite Fricke gel (NC-FG) dosimeter succeeded in complete suppression of diffusion. Surprisingly, we also found that the NC-FG dosimeter exhibited the response almost independent of LET. Further, its radiation response was nearly linear up to at least 800 Gy.

2. Experimental

2.1. Sample preparation

Sample of the NC-FG and the Fricke xylenol orange gel (FXG) dosimeters were used in this study. The NC-FG was composed of 1% (w/w) nanoclay (synthetic hectorite, or Laponite XLG; Rockwood Ltd), 3% (w/w) gelatin (300 g Bloom from porcine skin; Sigma-Aldrich), 1 mM ammonium iron(II) sulfate and 50 mM perchloric acid. The procedure for the preparation of NC-FG was as follows: first, the ultra-pure water was exposed to N_2O gas via 30 min bubbling to exclude dissolved oxygen. Subsequently, under stirring, gelatin and Laponite XLG were added to this ultra-pure water, followed by heating until dissolution to obtain a uniform dispersion state. Finally, 5% (w/w) aqueous Fricke stock solution (Fricke and Hart, 1966) was added at around 40 °c. Thus the prepared NC-FG was sealed into color comparison tubes, made of Pyrex glass (Iwaki Glass Co), as shown in Fig. 1 and was refrigerated to gelation for a day after preparation.

The FXG was prepared as previously described in the literature (Kron et al., 1997; Rae et al., 1996) using 5% (w/w) gelatin, 1 mM ammonium iron (II) sulfate, 50 mM sulfuric acid and 0.5 mM xylenol orange.

2.2. Irradiation

The irradiation experiments were performed at Biological Irradiation Port of Heavy Ion Medical Accelerator in Chiba (HIMAC), National Institute of Radiological Sciences (NIRS). A carbon ion beam at 290 MeV/nucleon with an irradiation field having $\pm 5\%$ lateral dose uniformity within a diameter of 10 cm was used. The radiation doses on the surface of the samples were controlled by the dose monitor that is an ionization chamber and located in the upper beam line (Kanai et al., 2004; Torikoshi et al., 2007). The monitor unit (MU) value was calibrated by using the Markus ionization chamber at the same position of samples. The depth-dose distribution of a carbon-ion beam in this system is reported in the literature (Kanai et al., 1999). The dose rate on the incident surface of the present experiments was 7–8 Gy/min. Simultaneous irradiation of multiple gel samples was performed from the bottoms of the color comparison tubes in the radiation field. The irradiation dose is summarized in Table 1.

2.3. MRI measurements

An 1.5T MRI scanner (Intera Achieva 1.5T HP Nova Dual Gradient, Philips Medical Systems, Best, The Netherlands) was used for the measurement of these samples. The longitudinal MR relaxation rate ($R_1 = 1/T_1$) of the samples was evaluated by using a turbo mixed sequence (Baldock et al., 1998; Denkleef and Cuppen, 1987). The conditions of the T_1 measurements were: TR = 2260 ms; $TE_1 = 19$ ms $TE_2 = 100$ ms; TI = 500 ms; ETL = 12; pixel spacing = 0.78 mm. The elapsed days after the sample irradiation for the MRI measurements are summarized in Table 1.

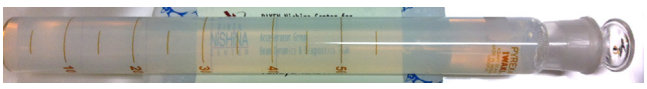

Fig. 1. Photograph of a deaerated NC-FG gel dosimeter.

Table 1
Irradiation surface doses and time of measurements for all gel dosimeters.

	Dose [Gy]	Elapsed days
NC-FG	200, 400, 600, 800	3, 9
FXG	0, 30	7

3. Results

3.1. Characteristics of NC-FG

An example of the R_1 ($1/T_1$) distributions measured for the FXG and the NC-FG irradiated with a 290 MeV/nucleon carbon beam is shown in Fig. 2. Fig. 2(a) and (b) refer to the FXG at 30 Gy and the NC-FG at 200 Gy, respectively. The NC-FG showed a very sharp peak near 140 mm, compared to the FXG. Given that the bottom of the color comparison tube which corresponds to the irradiation surface was not exactly flat, the distribution appears slightly curved in the y-axis direction. Further, the black part at the rightmost region (high region of R_1) represents the contamination of oxygen from the glass cap, causing autoxidation; however, it was confirmed that this black part did not spread thereafter.

Fig. 3 shows the R_1 increment ($R_1 - R_1(0)$) of the NC-FGs after irradiation with 200, 400, 600, 800 Gy. The R_1 value at the region with almost no dose contribution after the peak of each sample (around 190 mm), is used as $R_1(0)$. From Fig. 3, similar sharp distributions can be seen when the radiation dose was increased from 200 Gy to 800 Gy. The conventional Fricke gel dosimeters has a saturated dose response at 100 Gy (Schulz et al., 1990) and for the Fricke aqueous dosimeter this is reported to be 400 Gy (Matthews, 1982); above these values the linearity of dose response is lost due to the lack of Fe(II). Despite the very high dose at 4 kGy in the Bragg peak region, the peak observed for the 800 Gy incident dose shows the very sharp distribution similar to the 200 Gy incident dose, indicating that the progression of oxidation reaction of Fe(II) for absorbed dose is smaller than the conventional Fricke dosimeters.

In order to evaluate the dose dependence of the NC-FG, the $R_1 - R_1(0)$ values at various penetration depths were plotted in Fig. 4 as a function of the incident dose. The peak position near 141 mm for each sample differed to a small degree within MRI resolution (1 mm); hence, a minor correction was introduced in the direction of the penetration depth to adjust the peak position of each sample. From Fig. 4, a good linearity was confirmed at every position.

From the slopes of the dose-dependence curves in Fig. 4, the rate of R_1 increment (δR_1) per unit of entrance surface dose was evaluated and is plotted in Fig. 5. The δR_1 distributions after 3 days (dotted line) and 9 days (solid line) in Fig. 5 rendered very good consistency; it was found that the distribution did not change with time, implying that the diffusion of the product after irradiation was completely suppressed.

On the other hand, looking at the δR_1 distribution of the FXG gel dosimeter without the addition of nanoclay, there is almost no peak in its δR_1 distribution (right vertical axis in Fig. 5), presumably due to the reduction in dose response associated with increasing LET, and the diffusion of the radiation product.

The sensitivities of FXG and NC-FG near the entrance surface were 20 s^{-1} kGy^{-1} and 0.55 s^{-1} kGy^{-1}, respectively. It was found

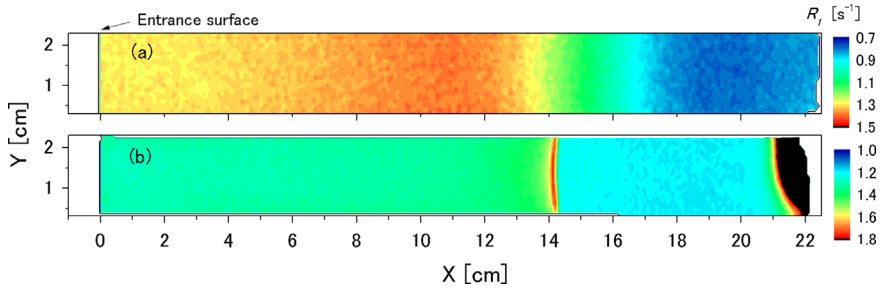

Fig. 2. R_1 distribution measured with MRI after irradiation with a 290 MeV/nucleon carbon beam for (a) FXG at 30 Gy and (b) NC-FG at 200 Gy.

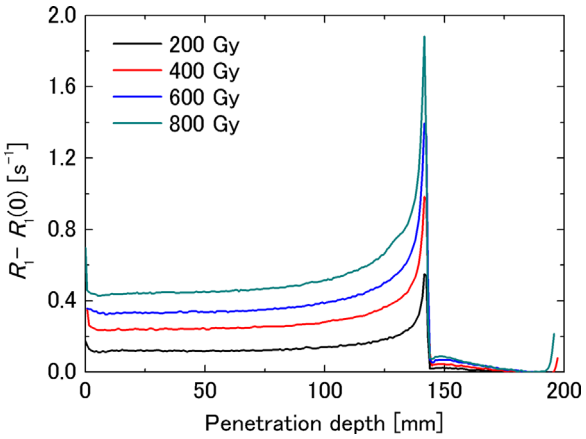

Fig. 3. $R_1 - R_1(0)$ distribution in the NC-FG dosimeters after irradiation with a 290 MeV/nucleon carbon beam at four different incident doses indicated in the figure.

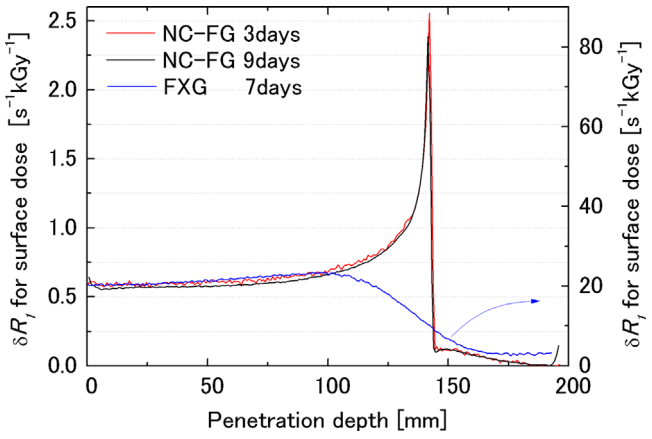

Fig. 5. The distribution of the carbon dose response δR_1 for FXG and NC-FG after the indicated elapsed days.

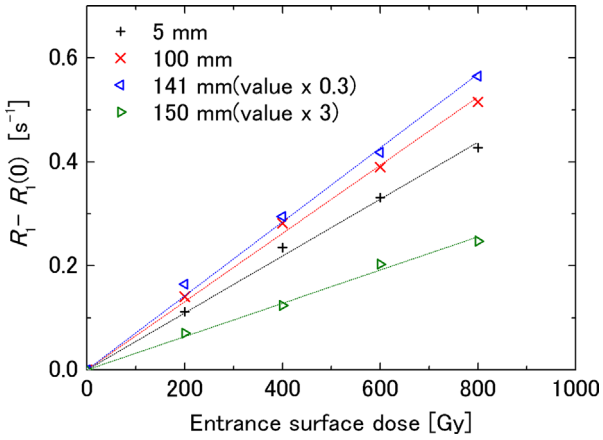

Fig. 4. $R_1 - R_1(0)$ in NC-FG vs. entrance surface dose at four different depths from the entrance surface.

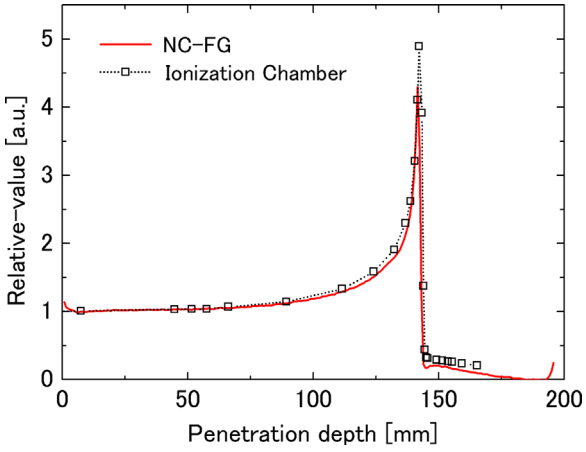

Fig. 6. Comparison between the δR_1 distribution of NC-FG and physical dose distribution measured with the ionization chamber. The curve for the latter has been shifted to the left by 5.7 mm in such a way that the peak positions match each other. The amount of the shift is accounted for mainly by the range shift due to the bottom thickness (2.1 mm) of the Pyrex tube (density 2.2 g/cm^3).

that the sensitivity of the NC-FG was only 1/40th that of the FXG dosimeter.

3.2. Comparison with physical dose distribution

In order to determine the LET dependence of the radiation sensitivity of the NC-FG, the δR_1 distribution and the dose distribution measured by the ionization chamber were compared in Fig. 6. The values of near surfaces (5–10 mm) for both the δR_1 distribution and the dose distribution were normalized. Also, the peak positions of the dose distribution were adjusted to having overlap with the peak positions of the δR_1 distribution. The peak enhancements (the rate of increase in peak with respect to the entrance surface) of the δR_1 distribution and dose distribution for NC-FG were 4.3 and 4.9, respectively. Since LET increases with the penetration depth, the physical dose gives a high dose locally at the range end (Bragg Peak). However, since the sensitivity of typical chemical dosimeters such as polymer gel dosimeters and Fricke aqueous dosimeters decreases by a factor of 2–3 with increasing LET in general, the dose at the Bragg peak is underestimated by the same factor compared with the entrance dose (Baker et al., 2009; Gustavsson et al., 2004; Heufelder et al., 2003; Kantemiris and et al., 2009; Ramm et al., 2004, 2000; Yates et al., 2011). In Fig. 6, in great contrast, the δR_1 distribution of NC-FG faithfully reproduces the dose distribution including the peak, indicating that the sensitivity of the NC-FG barely changes with LET. We have confirmed from our preliminary survey that this

property is retained also when Ar gas is used instead of N_2O gas or when the nanoclay concentration is decreased to 0.5% (w/w).

4. Discussion

4.1. Mechanism of diffusion suppression

In this study, we succeeded in complete suppression of diffusion of the radiation product by adding nano-sized clay (Laponite XLG) at a concentration as little as 1% (w/w). The expected effect of incorporating nanoclay into aqueous solution is the adsorption of anions onto the Laponite crystal edge and the adsorption of cations into the interlayer of nanoclay via the ion exchange reaction (Swartzen and Matijevi, 1974). Indeed, we have previously reported that the dichromate anion does not diffuse in the nanocomposite gel and that the neutral complex formed by Fe^{3+} and xylenol orange diffuses under the existence of nanoclay (Maeyama et al., 2012). On the other hand, in the present study, a plausible mechanism for the diffusion suppression is that the Fe^{3+} cations are incorporated into the interlayer of clay via a cation exchange reaction.

4.2. Mechanism of LET effects suppression

Let us discuss a possible mechanism underlying the suppression of LET dependence in NC-FG, starting from the LET effect on the radiolysis of water, which is the main component of the gel dosimeter. It is well-known that the radical-radical combination reaction increases with LET, leading to reduction in radical products (e.g., $^{\bullet}OH$ and $^{\bullet}H$) that otherwise contribute to the oxidation reaction in Fricke dosimetry system, and increase in molecular products (e.g., H_2O_2, H_2, O_2) (LaVerne, 2000). Hence, the dose sensitivity of the conventional Fricke gels (Back et al., 1999; DiCapua et al., 1997) and aqueous Fricke dosimeters (LaVerne and Schuler, 1996) decreases with LET. Among the molecular products, in particular, oxygen molecules generated through oxygen atoms formed in dissociation reaction of multiple ionization of water molecule (H_2O^{2+}),

$$H_2O^{2+} + 2H_2O \rightarrow 2H_3O^{+} + {}^{\bullet}O \quad (1)$$

$$^{\bullet}O + {}^{\bullet}O \rightarrow O_2 \quad (2)$$

increase with LET (Baverstock and Burns, 1981; Gervais et al., 2006; Gervais et al., 2005; Meesungnoen et al., 2003; Meesungnoen and Jay-Gerin, 2005, 2009).

It is reasonable to assume that a similar reduction in radical products and increase in molecular products also happens in gel. Although Fe^{2+} is oxidized even in the absence of O_2 in the aqueous Fricke solution, it is reported that the presence of O_2 is indispensable for the oxidation of Fe^{2+} to Fe^{3+} in the Fricke gel through the following chain reaction with the organic gel macromolecule (RH) (Appleby et al., 1988):

$$RH + {}^{\bullet}OH \rightarrow R^{\bullet} + H_2O \quad (3)$$

$$RH + H^{\bullet} \rightarrow R^{\bullet} + H_2 \quad (4)$$

$$R^{\bullet} + O_2 \rightarrow RO_2^{\bullet} \quad (5)$$

$$RO_2^{\bullet} + H^{+} + Fe^{2+} \rightarrow Fe^{3+} + RO_2H \quad (6)$$

$$RO_2H + Fe^{2+} \rightarrow Fe^{3+} + RO^{\bullet} + OH^{-} \quad (7)$$

$$RO^{\bullet} + RH \rightarrow {}^{\bullet}R + ROH \quad (8)$$

where most of the radicals (OH, H) produced in the radiolysis of water react with gel macromolecule (RH) [Eqs. (3) and (4)]. Thus, the amount of O_2 has a significant impact on the sensitivity of Fricke gel. We speculate that the decrease in radical products is compensated by the chain reaction [Eqs. (5) and (8)] promoted by the molecular O_2, which leads to the suppression of the LET dependence of the sensitivity.

An enhancement of dose-response by O_2 is also known for the aqueous Fricke solution, though less effective (~twice) and through reactions different from Eqs. (5) and (8). This may explain the large difference in sensitivity between the deaerated Fricke gel and the aerated Fricke gel seen in Fig. 5.

5. Conclusion

By incorporation of nano-sized clay particles and deaeration, we successfully suppressed the two main drawbacks, i.e., the diffusion of the radiation product and the LET-dependent sensitivity of Fricke gel dosimeters, irradiated by a 290 MeV/nucleon carbon-ion beam. The R_1 distribution measured by MRI showed virtually no diffusion for nine days after irradiation, probably due to the adsorption of Fe^{3+} cations to clay nanoparticles by a cation exchange reaction. A possible mechanism underlying the surprising absence of the LET dependence is the compensation of the decrease in radical products by the increase in O_2 production. Furthermore, the NC-FG system also exhibited a good linearity up to an incident dose of 800 Gy. The nanocomposite Fricke gel appears to be promising for 3D dose imaging under ion-beam irradiation, with potential applications in ion-beam cancer therapy (Linz, 2012).

Acknowledgment

This research has been carried out as a Research Project with Heavy Ions at NIRS-HIMAC. This research was supported by Research and Development of the Next-Generation Integrated Simulation of Living Matter, which is a part of the development and use of the Next-Generation Supercomputer Project of MEXT, Japan, as well as by RIKEN President's Discretionary Fund (Strategic Programs for R&D). TF and TM gratefully acknowledge support by the RIKEN Special Postdoctoral Researchers Program. TM also acknowledges support by The Grant-in-Aid for Young Scientists (B-16310036).

References

Appleby, A., Leghrouz, A., Christman, E.A., 1988. Radiation chemical and magnetic resonance studies of aqueous agarose gels containing ferrous ions. International Journal of Radiation Applications and Instrumentation Part C: Radiation Physics and Chemistry 32, 241–244.

Back, S.A., Medin, J., Magnusson, P., Olsson, P., Grusell, E., Olsson, L.E., 1999. Ferrous sulphate gel dosimetry and MRI for proton beam dose measurements. Physics in Medicine and Biology 44, 1983–1996.

Baker, C.R., Quine, T.E., Brunt, J.N.H., Kacperek, A., 2009. Monte Carlo simulation and polymer gel dosimetry of 60 MeV clinical proton beams for the treatment of ocular tumours. Applied Radiation and Isotopes 67, 402–405.

Baldock, C., Burford, R.P., Billingham, N., Wagner, G.S., Patval, S., Badawi, R.D., Keevil, S.F., 1998. Experimental procedure for the manufacture and calibration of polyacrylamide gel (PAG) for magnetic resonance imaging (MRI) radiation dosimetry. Physics in Medicine and Biology 43, 695–702.

Baldock, C., De Deene, Y., Doran, S., Ibbott, G., Jirasek, A., Lepage, M., McAuley, K.B., Oldham, M., Schreiner, L.J., 2010. Polymer gel dosimetry. Physics in Medicine and Biology 55, R1–R63.

Baverstock, K.F., Burns, W.G., 1981. Oxygen as a product of water radiolysis in high-let tracks. 2. Radiobiological implications. Radiation Research 86, 20–33.

Denkleef, J., Cuppen, J.J.M., 1987. RLSQ: T1, T2, and rho calculations, combining ratios and least squares. Magnetic Resonance in Medicine 5, 513–524.

DiCapua, S., DErrico, F., Egger, E., Guidoni, L., Luciani, A.M., Rosi, A., Viti, V., 1997. Dose distribution of proton beams with NMR measurements of Fricke-agarose gels. Magnetic Resonance Imaging 15, 489–495.

Fricke, H., Hart, E.J., 1966. Chemical Dosimetry. Academic Press.

Fricke, H., Morse, S., 1927. The chemical action of roentgen rays on dilute ferrosulphate solutions as a measure of dose. American Journal of Roentgenology and Radium Therapy 18, 430–432.
Gervais, B., Beuve, M., Olivera, G.H., Galassi, M.E., 2006. Numerical simulation of multiple ionization and high LET effects in liquid water radiolysis. Radiation Physics and Chemistry 75, 493–513.
Gervais, B., Beuve, M., Olivera, G.H., Galassi, M.E., Rivarola, R.D., 2005. Production of HO2 and O-2 by multiple ionization in water radiolysis by swift carbon ions. Chemical Physics Letters 410, 330–334.
Gore, J.C., Kang, Y.S., Schulz, R.J., 1984. Measurement of radiation-dose distributions by nuclear magnetic-resonance (Nmr) imaging. Physics in Medicine and Biology 29, 1189–1197.
Gustavsson, H., Bjack, S.A.J., Medin, J., Grusell, E., Olsson, L.E., 2004. Linear energy transfer dependence of a normoxic polymer gel dosimeter investigated using proton beam absorbed dose measurements. Physics in Medicine and Biology 49, 3847–3855.
Heufelder, J., Stiefel, S., Pfaender, M., Ludemann, L., Grebe, G., Heese, J., 2003. Use of BANG (R) polymer gel for dose measurements in a 68 MeV proton beam. Medical Physics 30, 1235–1240.
Kanai, T., Endo, M., Minohara, S., Miyahara, N., Koyama-Ito, H., Tomura, H., Matsufuji, N., Futami, Y., Fukumura, A., Hiraoka, T., Furusawa, Y., Ando, K., Suzuki, M., Soga, F., Kawachi, K., 1999. Biophysical characteristics of HIMAC clinical irradiation system for heavy-ion radiation therapy. International Journal of Radiation Oncology Biology Physics 44, 201–210.
Kanai, T., Fukumura, A., Kusano, Y., Shimbo, M., Nishio, T., 2004. Cross-calibration of ionization chambers in proton and carbon beams. Physics in Medicine and Biology 49, 771–781.
Kantemiris, I., et al., 2009. Carbon beam dosimetry using VIP polymer gel and MRI. Journal of Physics: Conference Series 164, 012055.
Karger, C.P., Jakel, O., Palmans, H., Kanai, T., 2010. Dosimetry for ion beam radiotherapy. Physics in Medicine and Biology 55, R193–R234.
Kron, T., Jonas, D., Pope, J.M., 1997. Fast T1 imaging of dual gel samples for diffusion measurements in NMR dosimetry gels. Magnetic Resonance Imaging 15, 211–221.
LaVerne, J.A., 2000. Track effects of heavy ions in liquid water. Radiation Research 153, 487–496.
LaVerne, J.A., Schuler, R.H., 1996. Radiolysis of the Fricke dosimeter with Ni-58 and U-238 ions: Response for particles of high linear energy transfer. Journal of Physical Chemistry 100, 16034–16040.
Linz, U., 2012. Ion Beam Therapy: Fundamentals, Technology, Clinical Applications. Springer, Berlin Heidelberg.
Maeyama, T., Fukunishi, N., Ishikawa, K.L., Fukasaku, K., Furuta, T., Takagi, S., Noda, K., Himeno, R., 2012. Diffusion suppression in gel dosimetry by addition of nanoclay. IFMBE Proceedings 39, 1183–1186.
Maeyama, T., Fukunishi, N., Ishikawa, K.L., Fukasaku, K., Furuta, T., Takagi, S., Noda, S., Himeno, R., Fukuda, S., 2013. Response of aqueous dichromate and nanoclay dichromate gel dosimeters to carbon ion irradiation. Journal of Physics: Conference Series 444, 012033.
Matthews, R.W., 1982. Aqueous chemical dosimetry. International Journal of Applied Radiation and Isotopes 33, 1159–1170.
Meesungnoen, J., Filali-Mouhim, A., Snitwongse, N., Ayudhya, N., Mankhetkorn, S., Jay-Gerin, J.P., 2003. Multiple ionization effects on the yields of HO2 center dot/O-2(center dot)- and H2O2 produced in the radiolysis of liquid water with high-LET C-12(6+) ions: a Monte-Carlo simulation study. Chemical Physics Letters 377, 419–425.
Meesungnoen, J., Jay-Gerin, J.P., 2005. High-LET radiolysis of liquid water with H-1(+), He-4(2+), C-12(6+), and Ne-20(9+) ions: effects of multiple ionization. Journal of Physical Chemistry A 109, 6406–6419.
Meesungnoen, J., Jay-Gerin, J.P., 2009. High-LET ion radiolysis of water: oxygen production in tracks. Radiation Research 171, 379–386.
Penev, K., Mequanint, K., 2013. The effect of mixed dopants on the stability of Fricke gel dosimeters. Journal of Physics: Conference Series 444, 012105.
Rae, W.I.D., Willemse, C.A., Lotter, M.G., Engelbrecht, J.S., Swarts, J.C., 1996. Chelator effect on ion diffusion in ferrous-sulfate-doped gelatin gel dosimeters as analyzed by MRI. Medical Physics 23, 15–23.
Ramm, U., Moog, J., Spielberger, B., Bankamp, A., Botcher, H.D., Kraft, G., 2004. Investigations of dose response of BANG (R) polymer-gels to carbon ion irradiation. Radiotherapy & Oncology 73, S99–S101.
Ramm, U., Weber, U., Bock, M., Kramer, M., Bankamp, A., Damrau, M., Thilmann, C., Bottcher, H.D., Schad, L.R., Kraft, G., 2000. Three-dimensional BANG (TM) gel dosimetry in conformal carbon ion radiotherapy. Physics in Medicine and Biology 45, N95–N102.
Rockwood, 2013. Laponite® performance additives (Technical Brochure) [Available from: ⟨http://www.scprod.com/pdfs/laponite.pdf⟩]. Rockwood Ltd.
Schreiner, L.J., 2004. Review of Fricke gel dosimeters. Journal of Physics: Conference Series 3, 9–21.
Schulz, R.J., Deguzman, A.F., Nguyen, D.B., Gore, J.C., 1990. Dose-response curves for Fricke-Infused Agarose Gels as obtained by nuclear-magnetic-resonance. Physics in Medicine and Biology 35, 1611–1622.
Swartzen, Sl, Matijevi, E, 1974. Surface and colloid chemistry of clays. Chemical Reviews 74, 385–400.
Taylor, M.L., Maeyama, T., Fukunishi, N., Ishikawa, K.L., Fukasaku, K., Furuta, T., Takagi, S., Noda, S., Himeno, R., Fukuda, S., 2013. Radiological characteristics of charged particle interactions in the first clay-nanoparticle dichromate gel dosimeter. Journal of Physics: Conference Series 444, 012110.
Torikoshi, M., Minohara, S., Kanematsu, N., Komori, M., Kanazawa, M., Noda, K., Miyahara, N., Itoh, H., Endo, M., Kanai, T., 2007. Irradiation System for HIMAC. Journal of Radiation Research 48, A15–A25.
Yates, E.S., Balling, P., Petersen, J.B.B., Christensen, M.N., Skyt, P.S., Bassler, N., Kaiser, F.J., Muren, L.P., 2011. Characterization of the optical properties and stability of Presage (TM) following irradiation with photons and carbon ions. Acta Oncologica 50, 829–834.